MOTIVECTION
Journal of Mechanical Electrical and Industrial Engineering

Volume: 7, Number: 1, 2025
ISSN: 2655 – 7215 [printed]; 2685-2098 [online]
DOI: https://doi.org/10.46574/motivection.v7i1.427

Seismic Analysis of Minimum Separation Distance for Low-Rise Buildings in Padang City to Prevent Structural Collisions

Ardi Pratama[1], Masrilayanti[1]*, Ruddy Kurniawan[1], Risma Apdeni[2]

ABSTRACT

This study examines the minimum effective separation distance between buildings necessary to avert structural damage from building pounding in Padang City, an area particularly vulnerable to seismic events. The study examines 45 structures throughout five districts, classified into three categories according to their height-to-width (H/L) ratio: (0.5–1.0), (1.1–1.5), and (1.51–2.0). Three pairs of ground acceleration records—Imperial Valley-06, Tokachi-Oki Aftershock, and Tokachi-Oki Mainshock—were selected and calibrated to align with the target response spectrum of Padang City using linear time-history analysis. The research assesses structural displacement capacity and drift ratio to ascertain the necessary minimum separation distances. The findings reveal that the minimum separation distance for Category A (H/L: 0.5–1.0), Category B (H/L: 1.1–1.5), and Category C (H/L: 1.51–2.0) spans from 40 cm to 48.4 cm, with a suggested practical separation of 50 cm per building. A separation distance of 1 meter is recommended to reduce the risk of structural collisions during earthquakes. These findings serve as a technical reference for urban planners, engineers, and legislators, facilitating safer building designs, enhanced seismic resilience, and diminished structural damage in earthquake-prone regions.

Keywords
Building Separation Distance, Building Impact Collisions, Time History Analysis, Structural Displacement

[1] Department of Civil Engineering, Faculty of Engineering, Universitas Andalas
Kampus Limau Manis, Pauh, Padang City, West Sumatra, INDONESIA
[2] Department of Civil Engineering, Faculty of Engineering, Universitas Negeri Padang
Jl. Prof. HAMKA, Air Tawar, Padang City, West Sumatra, INDONESIA
* Corresponding Author: masrilayanti@eng.unand.ac.id

Submitted : February 23, 2025. Accepted : March 16, 2025. Published : March 17, 2025

INTRODUCTION

In recent decades, Indonesia has experienced numerous strong earthquakes, with over 50% of the country at risk of significant damage. The rapid population growth and urban expansion have led to land scarcity, particularly in metropolitan areas [1]. To address this challenge, high-rise buildings are often constructed in close proximity, increasing the likelihood of pounding effects during earthquakes. Pounding effects refer to collisions between adjacent structures or impacts between different sections of the same building during seismic activity [2]. Although earthquakes remain unpredictable, their impact on the population can be significantly mitigated through appropriate and timely measures in response to ground movements [3]. Historical observations of seismic disasters reveal that reinforced concrete structures often incur significant damage not alone from structural load-bearing constraints but also from the impact of nearby building collisions. This problem occurs when safe separation distances are not accounted for in planning, potentially resulting in structural failure [4].

Pounding effects generally arise when structures with differing size and structural systems, possessing unique natural periods, demonstrate disparate seismic responses based on ground motion characteristics. Insufficient spacing between two buildings results in collisions, altering the dynamic response of both structures and putting extra inertial pressures on their systems [1]. This study focuses primarily on low-rise buildings, as these structures are often not properly planned, mainly due to limited technical knowledge and economic constraints within communities. As a result, their construction frequently relies on the experience of local builders rather than engineering expertise. Conversely, high-rise buildings are designed by skilled engineers, ensuring compliance with existing regulations and seismic safety standards. Nevertheless, the methodology used in this study has the potential to be extended to high-rise buildings, provided certain modifications are made to accommodate more complex structural planning requirements.

Insufficient separation between neighboring buildings can lead to collisions that significantly damage both structural and non-structural components, causing economic losses and diminishing urban resilience in the aftermath of an earthquake [4]. Numerous contemporary seismic codes delineate minimum separation distances to prevent building collisions [5]. Nevertheless, numerous countries lack explicit rules for establishing suitable separation lengths based on seismic behavior. Previous studies have extensively explored the relationship between pounding effects and soil type parameters, as demonstrated in research conducted by Miari, Choong, & Jankowski [6], Tena-Colunga & Sánchez-Ballinas [7], and Miari & Jankowski [8].

These investigations commonly reveal that more rigid soil categories correlate with increased structural displacements. Additional study indicates that the impact of pounding can be alleviated by integrating energy absorbers, including springs and viscoelastic dampers, into architectural designs. The longitudinal reaction of a structure is considerably affected by impact forces, but the transverse response is negligible due to frictional forces operating in the transverse direction. As separation distances augment, impact pressures diminish, therefore lessening harm to neighboring structures [9]. Implementing dampening systems in basic structures in Padang City is impossible due to exorbitant costs and a lack of competent staff. Consequently, the most pragmatic strategy is to implement a minimum separation guideline for low-rise buildings. Due to the unpredictability of damage caused by earthquakes, such as structural collapse, financial losses, and fatalities, comprehensive seismic mitigation strategies are crucial to reduce the effects of disasters [10].

Padang City is acknowledged as a place with a high susceptibility to earthquakes, often resulting in structural damage post-seismic occurrences [11][12]. Consequently, it is imperative to evaluate separation lengths between structures to avert collapse resulting from pounding impacts. This concern is especially pertinent for uncomplicated residential structures and low-rise commercial edifices, where constructors frequently fail to ensure enough separation distances, hence heightening the risk of structural damage during seismic events. Data from the 2009 earthquake indicated that 135,448 dwellings were badly destroyed, 65,380 houses were moderately damaged, and 78,604 houses experienced minor damage. A considerable amount of this damage transpired in low-rise structures, underscoring residential zones as the most susceptible sector in Padang City [13]. Accordingly, This study seeks to assess the impact of building slenderness on establishing minimum separation distances between existing and future structures to reduce damage from pounding impacts in Padang City. The study utilizes time-history analysis with ground acceleration records, a structural analysis method that elucidates building behavior during seismic events. This approach employs earthquake ground motion data to replicate genuine seismic conditions. This study primarily

analyzes structural displacement, utilizing SeismoStruct 2022 software to model and simulate current building structures.

METHOD

Data Collection

The data collection process involved gathering information on building locations, beam and column dimensions, column spacing, building heights, types of reinforcement, and concrete quality. This data was obtained from a previous study titled "Evaluation of the Structural Performance of Existing Shop-House Buildings in Earthquake-Prone Areas" conducted by Chairunnisa [14]. The survey in the referenced study was conducted across various districts in Padang City, including Kuranji, Lubuk Begalung, Nanggalo, Padang Barat, Padang Selatan, Padang Timur, Koto Tangah, Pauh, and Padang Utara, with a total sample of 45 buildings.

Building Sample Classification

The prior study initially identified 45 building examples; however, when examining the height-to-width ratio (H/L), samples with equal slenderness ratios were removed, resulting in a total of 28 samples remaining. The samples were categorized into four groups according to their H/L values: Category 1 included buildings with a H/L ratio of 0.5 to 1, Category 2 encompassed buildings with a H/L ratio of 1.1 to 1.5, Category 3 contained those with a H/L ratio of 1.51 to 2, and Category 4 consisted of buildings with a H/L ratio exceeding 2. The reinforcement requirements utilized in this study were derived from the average forms of reinforcement often used in the construction of simple multi-story dwellings in Padang City, as established by survey data. The concrete strength values for analysis were obtained from hammer test results performed during the survey, ensuring that the material attributes accurately represented the real conditions in the research area.

Selection of Ground Motions

The time-history analysis approach necessitates that the chosen seismic inputs (accelerograms) precisely reflect ground motion recordings from earthquakes pertinent to the study area, taking into account variables such as earthquake magnitude and proximity to the seismic source. This study's selection of earthquake data according to SNI 1726:2019 Article 7.9.2.3, which outlines the criteria for assessing seismic loads and adjusting ground motions according to regional attributes. The seismic data utilized in this research were sourced from the Indonesian Earthquake Hazard Deaggregation Map for Earthquake-Resistant Infrastructure Planning and Evaluation (2022).

RESULT

The data that will be used to determine seismic loads for the linear time-history analysis are presented in Table 1.

Table 1. Ground Motion Selection Criteria

Source	Magnitude			Distance (Km)		
	PGA	0,2 sec	3 sec	PGA	0,2 sec	3 sec
Shallow Crustail		6.4-6.6			20-30	
Benioff		7.2-7.4			80-100	
Megatruss		8.4-8.6			70-80	

Return Period	1000	Year
Location	Padang	
Site Class	Medium Soil (SD)	
VS	175-350	m/s

Once the required data was collected, it was processed using the PEER Ground Motion Database search engine. This database facilitates the identification of ground motion records that align with specific selection criteria, including earthquake magnitude, source distance, and site characteristics. The selected ground motion records were then analyzed to ensure compatibility with the study parameters. The results of the search process are presented in Table 2.

Table 2. Results from PEER Ground Motion Database Search

RSN	Event	Location	Year	M	R (Km)	VS-30
176	Imperial Valley-06	California	1979	6,53	21,98	249,92
4028843	Tokachiokiaft	Japan	2003	7,37	83,0	275,2
4028585	Tokachi-oki	Japan	2003	8.29	79	22,7

The selected records have been scaled to match the target spectrum for Padang City, ensuring compatibility with local seismic characteristics as outlined in SNI 1726:2019. These ground motion records will serve as the input for the linear time-history analysis in this study.

Spectral Matching

The next step involved matching the obtained ground motion data using SeismoMatch software. The process began by inputting the target spectrum, which corresponds to the response spectrum for Padang City derived from the initial calculations. Subsequently, the earthquake data acquired from the PEER Ground Motion Database was uploaded into the software for further analysis. The procedure is illustrated in Figure 1.

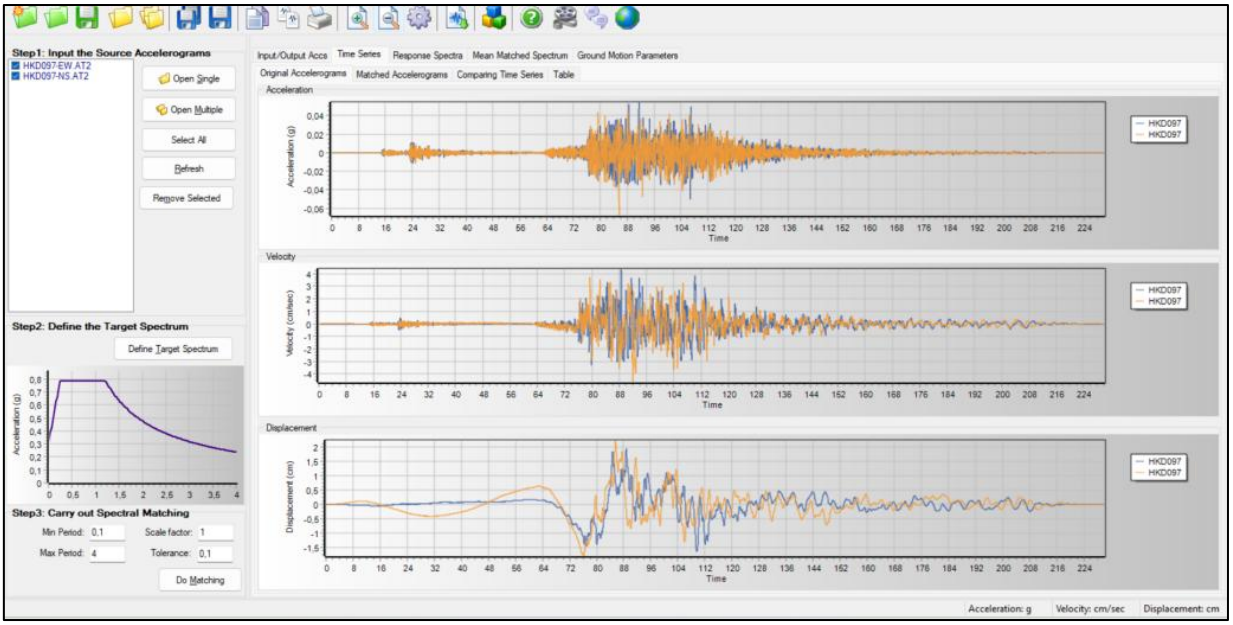

Figure 1. Spectral Matching

Figure 1 depicts the procedure of correlating earthquake data from the PEER Ground Motion Database with the response spectrum of Padang City. The first column illustrates the acceleration matching process, the second column displays the velocity matching process, and the third column indicates the displacement matching process. This stage is essential to guarantee that the chosen ground motion records adequately represent the seismic attributes of Padang City, thus facilitating a more dependable structural response analysis under earthquake loading.

According to the provisions outlined in SNI 1726:2019 Article 7.9.2.3.1, the maximum allowable average error in the analysis must remain within ±10% of the target response spectrum, meaning it should fall within the range of 90–110% of the target response spectrum. This requirement can be validated during the matching process, as demonstrated in Figure 2.

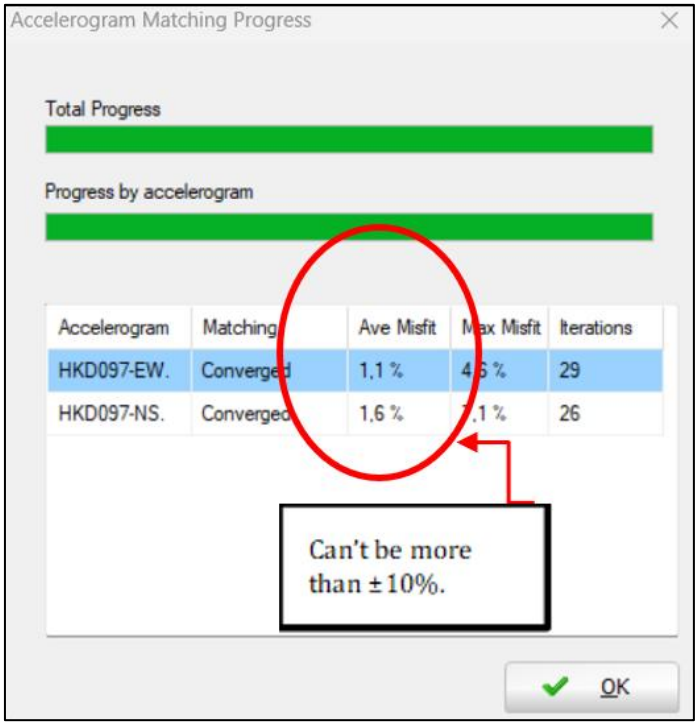

Figure 2. Max error Average from analysis.

The data obtained from SeismoMatch must then be filtered by extracting only the Time and Acceleration values. This ensures compatibility for input into the Linear Time History Analysis using SeismoStruct 2022.

Building Modeler

Data of 3-storey buildings that were research samples and have been grouped into 4 categories, and also data of reinforcement and concrete quality used are shown in Table 3, 4, and 5 respectively.

Table 3. Data on 3-Story Buildings in Padang City

Code	Floor Height	Total Height H (m)	Number of Portals	Portal Distance	Width L (m)	Cross-Section (m)		H/L
						Column	Beam	0,51-1,0
A1	2.5	7.5	3	4.3	12.9	42 x 42	25 x 30	0.58
A2	3	9	3	4.7	14.1	35 x 35	30 x 40	0.64
A3	4	12	4	4.6	18.4	36 x 36	25 x 30	0.65

A4	3	9	4	3	12	26 x 26	26 x 30	0.75
A5	3.4	10.2	3	4	12	30 x 30	24 x 30	0.85
A6	4.3	12.9	3	4.7	14.1	36 x 36	25 x 30	0.91
A7	3.8	11.4	3	4	12	28 x 28	24 x 30	0.95
A8	3.4	10.2	3	3.5	10.5	24 x 28	20 x 30	0.97
A9	4	12	3	4	12	25 x 25	25x30	1.00
Code	Floor Height	Total Height H (m)	Number of Portals	Portal Distance	Width L (m)	Cross-Section (m)		H/L
						Column	Beam	1,1-1,5
B1	3.5	10.5	2	5	10	42 x 42	30 x 40	1.05
B2	3.5	10.5	2	4.5	9	29 x 29	27 x 29	1.17
B3	3	9	2	3.8	7.6	30 x 30	25 x 30	1.18
B4	4.5	13.5	3	3.6	10.8	40 x 40	30 x 30	1.25
B5	3	9	2	3.5	7	34 x 34	23 x 30	1.29
B6	3.8	11.4	2	4.2	8.4	30 x 30	30 x 40	1.36
B7	3.5	10.5	2	3.7	7.4	36,5x36,5	20 x 30	1.42
B8	3.8	11.4	2	4	8	25 x 25	25 x 30	1.43
B9	3	9	2	3.1	6.2	39 x 39	20 x 30	1.45
B10	4	12	2	4	8	30 x 30	30 x 35	1.50
Code	Floor Height	Total Height H (m)	Number of Portals	Portal Distance	Width L (m)	Cross-Section (m)		H/L
						Column	Beam	1,51-2,0
C1	3.5	10.5	2	3.3	6.6	30 x 30	20 x 25	1.59
C2	4	12	2	3.6	7.2	30 x 30	25 x 30	1.67
C3	4	12	2	3.5	7	24 x 24	20 x 24	1.71
C4	3	9	2	2.5	5	30 x 30	25 x 30	1.80
C5	3	9	1	5	5	38 x 38	20 x 30	1.80
C6	4.5	13.5	2	3.5	7	30 x 30	25 x 30	1.93
Code	Floor Height	Total Height H (m)	Number of Portals	Portal Distance	Width L (m)	Cross-Section (m)		H/L
						Column	Beam	2 >
D1	4	12	1	5.5	5.5	30 x 30	30 x 35	2.18
D2	3	9	1	3.4	3.4	35 x 35	30 x 35	2.21
D3	3.5	11.5	1	4	4	35 x 35	35 x 30	2.88

Based on field inspection results, the average reinforcement ratio for residential buildings in Padang City was found to be approximately 1.4% for beam reinforcement and ±2% for column reinforcement. Therefore, all building models in this study were designed using these reference reinforcement ratios to ensure consistency with actual construction practices. The following section presents the calculated reinforcement results for beams and columns.

Table 4. Reinforcement Data

Code	Cross-Section (m)					
	Column	Reinforcement	Ratio (%)	Beam	Reinforcement	Ratio (%)
A1	42 x 42	12D19	2	25 x 30	8D13	1,4
A2	35 x 35	12D16	2	30 x 40	8D16	1,3
A3	36 x 36	14D16	2,2	25 x 30	8D13	1,4

Code	Cross-Section (m)					
	Column	Reinforcement	Ratio (%)	Beam	Reinforcement	Ratio (%)
A4	26 x 26	10D13	2	26 x 30	8D13	1,4
A5	30 x 30	10D16	2,2	24 x 30	8D13	1,3
A6	36 x 36	14D16	2,2	25 x 30	8D13	1,4
A7	28 x 28	8D16	2	24 x 30	8D13	1,4
A8	24 x 28	10D16	2	20 x 30	6D13	1,4
A9	25 x 25	10D13	2,2	25x30	8D13	1,4
Code	Cross-Section (m)					
	Columns	Reinforcement	Ratio (%)	Beam	Reinforcement	Ratio (%)
B1	42 x 42	12D19	2	30 x 40	8D16	1,3
B2	29 x 29	8D16	2	27 x 29	6D16	1,4
B3	30 x 30	10D16	2,2	25 x 30	8D13	1,4
B4	40 x 40	12D19	2,2	30 x 30	6D16	1,3
B5	34 x 34	12D16	2	23 x 30	8D13	1,5
B6	30 x 30	10D16	2,2	30 x 40	8D16	1,3
B7	36,5x36,5	14D16	2,1	20 x 30	6D13	1,4
B8	25 x 25	10D13	2,1	25 x 30	8D13	1,4
B9	39 x 39	10D16	2	20 x 30	6D13	1,4
B10	30 x 30	10D16	2,2	30 x 35	8D16	1,5
Code	Cross-Section (m)					
	Column	Reinforcement	Ratio (%)	Beam	Reinforcement	Ratio (%)
C1	30 x 30	10D16	2,2	20 x 25	4D13	1,1
C2	30 x 30	10D16	2,2	25 x 30	8D13	1,4
C3	24 x 24	10D13	2,2	20 x 24	4D13	1,1
C4	28 x 28	8D16	2,2	20 x 24	4D13	1,1
C5	30 x 30	10D16	2,2	25 x 30	8D13	1,4
C6	38 x 38	14D16	2	20 x 30	4D13	1,4
C7	30 x 30	10D16	2,2	25 x 30	8D13	1,4

The concrete quality used was determined from the average results of hammer test analyses conducted on several field samples, as can be seen in Table 5.

Table 5. Concrete Quality

Structural Element (Column)	Characteristic Compressive Strength Values (Mpa)
Sample 1	21,29
Sample 2	21,89
Sample 3	22,85
Average	**22,01**

Upon completing the Linear Time History analysis, the results obtained represent the displacement values derived from the earthquake records. The maximum displacement value at the observation point (δmax) is used for further analysis. These displacement values are then evaluated based on SNI 1726:2019, which governs structural separation requirements.

According to this regulation, the separation distance must accommodate the maximum inelastic response displacement (δM), which is determined by using Equation 1.

$$\delta_M = \frac{C_d \cdot \delta_{Max}}{I_e} \quad (1)$$

Where:

δ_{max} : Maximum elastic displacement at the critical location

C_d : Deflection amplification factor (5 ½ for reinforced concrete frames carrying special moment).

I_e : Earthquake importance factor (1 for Category II, which includes residential buildings).

These parameters will be used to determine the appropriate separation distance to accommodate the maximum inelastic response displacement and prevent structural pounding during an earthquake.

Building Performance Evaluation

The analysis begins by identifying the largest earthquake record to be used as the ground motion input for all building samples. This is achieved by applying each earthquake record to a single building model. In this study, sample A2 was selected for initial analysis, and the results are presented in Table 6.

Table 6. Displacement and Drift Ratio in Elastic Condition.

Number	Type of Earthquake	Displacement (cm)	Ratio Drift (%)
1	EW-Tokachiokiaft	3,8	0,42
2	NS-Tokachiokiaft	1,9	0,21
3	EW-Tokachi-oki	3,7	0,41
4	NS-Tokachi-oki	2,5	0,28
5	EW-Imperial Valley-06	2,5	0,28
6	NS-Imperial Valley-06	2,8	0,31

Subsequently, the displacement values were evaluated based on SNI 1726:2019, which regulates structural separation requirements. The separation distance must accommodate the maximum inelastic response displacement (δM), with the results detailed in Table 7.

Table 7. Displacement and Drift Ratio in Inelastic Condition.

Number	Type of Eartquake	Displacement (cm)	Ratio Drift (%)
1	EW-Tokachiokiaft	20,9	2,32
2	NS-Tokachiokiaft	10,45	1,16
3	EW-Tokachi-oki	20,35	2,26
4	NS-Tokachi-oki	2,5	1,53
5	EW-Imperial Valley-06	13,75	1,53
6	NS-Imperial Valley-06	15,4	1,71

For the Time History analysis, the most significant earthquake record chosen was Tokachi-Oki (East-West component). The analysis produced the following outcomes: elastic displacement of 3.8 cm, elastic drift ratio of 0.36%, inelastic displacement of 20.9 cm, and inelastic drift ratio of 2.33%. The values were employed to assess the building's performance

and ascertain the requisite structural separation to mitigate pounding impacts during an earthquake.

Time History Analysis

The next step involved performing a linear time history analysis on all building samples using the Tokachi-Oki (East-West component) earthquake record. The results of this analysis are presented in the Table 8.

Table 8. Displacement and Drift Ratio in Elastic Condition.

Code	Height H (m)	Width L (m)	Cross-Section (cm)		H/L	Maximum Displacement (cm)	Drift Ratio (%)
			Column	Beam	0,51-1		
A1	7,5	12,9	42 x 42	25 x 30	0,58	1,1	0,15
A2	9	14,1	35 x 35	30 x 40	0,64	3,8	0,29
A3	12	18,4	36 x 36	25 x 30	0,65	8,3	0,69
A4	9	12	26 x 26	26 x 30	0,75	5,7	0,63
A5	10,2	12	30 x 30	24 x 30	0,85	5,1	0,5
A6	12,9	14,1	36 x 36	25 x 30	0,91	8,8	0,68
A7	11,4	12	28 x 28	24 x 30	0,95	7,3	0,64
A8	10,2	10,5	24 x 28	20 x 30	0,97	5,7	0,56
A9	12	12	25 x 25	25x30	1,00	9,3	0,78
Code	Height H (m)	Width L (m)	Cross-Section (cm)		H/L	Maximum Displacement (cm)	Drift Ratio (%)
			Column	Beam	0,51-1		
B1	10,5	10	42 x 42	30 x 40	1,05	3,9	0,37
B2	10,5	9	29 x 29	27 x 29	1,17	7,5	0,71
B3	9	7,6	30 x 30	25 x 30	1,18	4,3	0,48
B4	13,5	10,8	40 x 40	30 x 30	1,25	6,8	0,5
B5	9	7	34 x 34	23 x 30	1,29	3,9	0,43
B6	11,4	8,4	30 x 30	30 x 40	1,36	5,1	0,45
B7	10,5	7,4	36,5x36,5	20 x 30	1,42	4,1	0,39
B8	11,4	8	25 x 25	25 x 30	1,43	10,1	0,89
B9	9	6,2	26 x 39	20 x 30	1,45	3,2	0,36
B10	12	8	30 x 30	30 x 35	1,50	6,9	0,58
Code	Height H (m)	Width L (m)	Cross-Section (cm)		H/L	Maximum Displacement (cm)	Drift Ratio (%)
			Column	Beam	0,51-1		
C1	10,5	6,6	30 x 30	20 x 25	1,59	6	0,57
C2	12	7,2	30 x 30	25 x 30	1,67	7,7	0,64
C3	12	7	24 x 24	20 x 24	1,71	10,3	0,86
C4	9	5	30 x 30	25 x 30	1,80	3,4	0,38
C5	9	5	38 x 38	20 x 30	1,80	4,8	0,53
C6	13,5	7	30 x 30	25 x 30	1,93	10,3	0,76

The Linear Time History analysis conducted with SeismoStruct yielded findings demonstrating good performance, with the drift ratios of all buildings remaining under the permissible limit of 2% of the total building height, as stipulated in SNI 1726:2019, Article 7.20.1. A capacity assessment of the structures will be performed, succeeded by an inelastic

analysis to ascertain the maximum inelastic displacement. These findings will act as a benchmark for establishing the necessary separation distance between structures to alleviate pounding impacts during an earthquake.

Analysis of Displacement and Drift Ratio in Inelastic Condition

Similar to the previous analysis, the displacement values were evaluated based on SNI 1726:2019 to determine the maximum inelastic displacement using Equation 1. Thus, from the analysis using the Equation 1, the following results were obtained as shown in Table 9.

Table 9. Displacement and Drift Ratio in Inelastic Condition

Code	Height H (m)	Width L (m)	Cross-Section (cm)		H/L	Maximum Displacement (cm)	Drift Ratio (%)
			Column	Beam	0,51-1		
A1	7,5	12,9	42 x 42	25 x 30	0,58	6,05	0,81
A2	9	14,1	35 x 35	30 x 40	0,64	20,9	2,32
A3	12	18,4	36 x 36	25 x 30	0,65	45,65	3,8
A4	9	12	26 x 26	26 x 30	0,75	31,35	3,48
A5	10,2	12	30 x 30	24 x 30	0,85	28,05	2,75
A6	12,9	14,1	36 x 36	25 x 30	0,91	48,4	3,75
A7	11,4	12	28 x 28	24 x 30	0,95	40,15	3,52
A8	10,2	10,5	24 x 28	20 x 30	0,97	31,35	3,07
Code	Height H (m)	Width L (m)	Cross-Section (cm)		H/L	Maximum Displacement (cm)	Drift Ratio (%)
			Column	Beam	0,51-1		
B1	10,5	10	42 x 42	30 x 40	1,05	21,45	2,04
B2	10,5	9	29 x 29	27 x 29	1,17	41,25	3,93
B3	9	7,6	30 x 30	25 x 30	1,18	23,65	2,63
B4	13,5	10,8	40 x 40	30 x 30	1,25	37,4	2,77
B5	9	7	34 x 34	23 x 30	1,29	21,45	2,38
B6	11,4	8,4	30 x 30	30 x 40	1,36	28,05	2,46
B7	10,5	7,4	36,5x36,5	20 x 30	1,42	22,55	2,15
B9	9	6,2	39 x 39	20 x 30	1,45	17,6	1,96
B10	12	8	30 x 30	30 x 35	1,50	37,95	3,16
Code	Height H (m)	Width L(m)	Cross-Section (cm)		H/L	Maximum Displacement (cm)	Drift Ratio (%)
			Column	Beam	0,51-1		
C1	10,5	6,6	30 x 30	20 x 25	1,59	33	3,14
C2	12	7,2	30 x 30	25 x 30	1,67	42,35	3,53
C4	9	5	30 x 30	25 x 30	1,80	18,7	2,08
C5	9	5	38 x 38	20 x 30	1,80	26,4	2,93%

To clearly display the variation in building displacement, the data is presented in Figure 3.

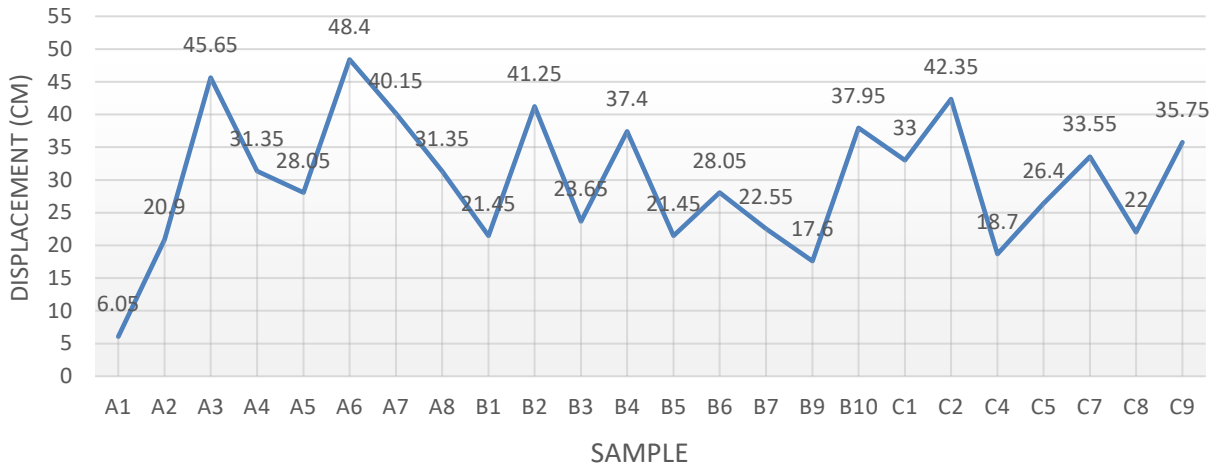

Figure 3. Displacement Curve.

The graph in Figure 3 illustrates the variation in displacement among building samples in Padang City, with the smallest displacement recorded for sample A1 at 6.08 cm, while the largest displacement was observed for sample A6 at 48.4 cm.

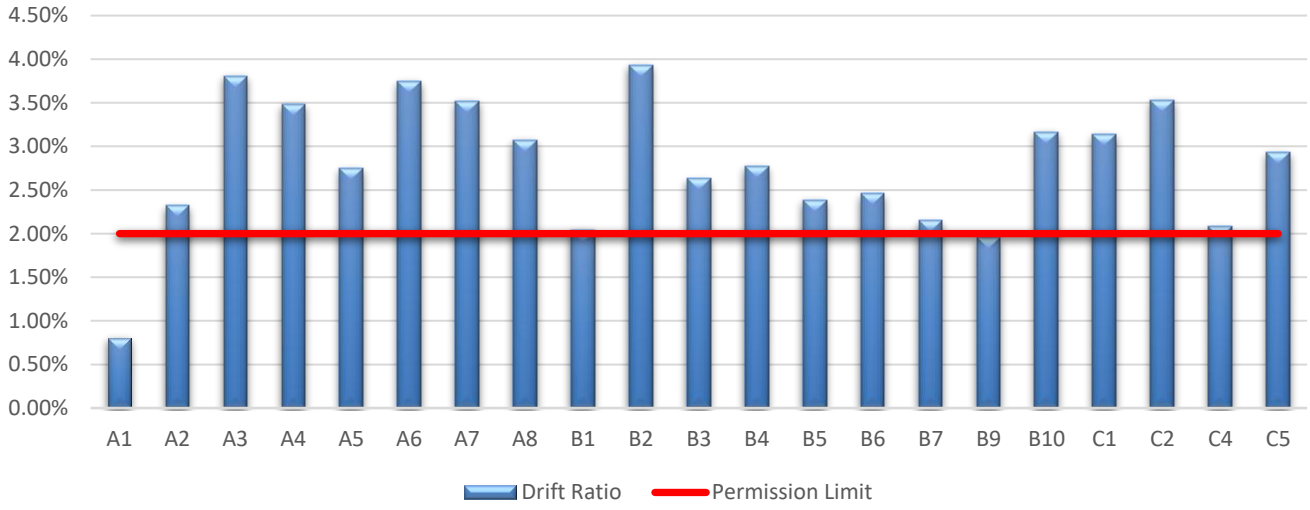

Figure 4. Drift Ratio Curve.

Meanwhile, Figure 4 presents the variation in drift ratio among the observed building samples. The smallest drift ratio was recorded for sample A1 at 0.81%, whereas the largest drift ratio was found in sample B2, reaching 3.93%.

DISCUSSION

This study seeks to ascertain the minimum separation distance between structures in Padang City by an investigation of structural responses to seismic loads. The method employed is linear time-history analysis, which evaluates the performance of 45 structures across five districts in Padang City. The analysis includes three pairs of ground acceleration records: Imperial Valley-06, Tokachi-Oki Aftershock, and Tokachi-Oki Mainshock, utilized as seismic inputs. The data were modified to align with the target response spectrum of Padang City, thereby correctly reflecting the local seismic characteristics.

The main factors examined are the structural element capacity regarding displacement and drift ratio. This methodology assesses probable interactions between neighboring buildings during earthquakes, ultimately determining a safe minimum separation distance within the study area. This methodology aims to deliver technical advice to enhance urban planning and seismic risk reduction initiatives in Padang City.

According to the analytical results for the H/L category of 0.5–1.0, sample BGNA6 (H/L 0.91) demonstrated a maximum displacement of 48.4 cm with a drift ratio of 3.48%, while sample BGNA8 (H/L 0.97) revealed a displacement of 31.35 cm with a drift ratio of 3.07%. This variation is due to the increased column height in BGNA6 (12.9 m) relative to BGNA8 (10.2 m), alongside the substantial disparity in ultimate moment capacity, with BGNA6 achieving 130.48 kNm and BGNA8 only 55.5 kNm. Therefore, for structures in this classification, the advised minimum separation distance is 48.4 cm.

In Category H/L 1.1–1.5, sample B2 (H/L 1.17) demonstrated a maximum displacement of 41.25 cm with a drift ratio of 3.93%, whereas sample B3 (H/L 1.18) recorded a displacement of 23.65 cm with a drift ratio of 2.63%. The discerned discrepancies can be ascribed to variances in column height (B2: 10.9 m vs. B3: 9 m), column cross-sectional dimensions (B2: 29×29 cm vs. B3: 30×30 cm), and ultimate moment capacity (B2: 54.39 kNm vs. B3: 42.4 kNm). Therefore, the advised minimum separation distance for this group is 41.4 cm.

In Category H/L 1.51–2.0, sample C2 (H/L 1.67) demonstrated a maximum displacement of 41.25 cm with a drift ratio of 3.53%, while sample C4 (H/L 1.71) recorded a displacement of 23.65 cm with a drift ratio of 2.63%. The disparities in displacement and drift ratio can be ascribed to variances in column height, cross-sectional dimensions, and column spacing (C2: 3.6 m vs. C4: 2.5 m). The maximal moment capacity of C2 is 42.27 kNm, but for C4, it is 56.21 kNm. The suggested minimum separation distance for this category is 42.35 cm.

The minimum distance between buildings must be established according to the maximum displacement value from each assessed category. The data indicates that the advised minimum separation distance for buildings in Padang City is 48.8 cm for Category H/L 0.5–1.0. These findings offer practical recommendations for planning building separations to reduce the risk of structural pounding and improve seismic safety.

CONCLUSION

Conclusion

The analysis indicates that the minimal separation distance for building categories A, B, and C is between 40 cm and 48.4 cm. A specified minimum separation distance of 50 cm per building is advised for practical implementation. To avert structural pounding between neighboring buildings in Padang City, a minimum separation distance of 1 meter is recommended. This study's findings underscore the essential influence of building slenderness and structural reaction on establishing safe separation distances, especially in seismically active areas. The linear time-history analysis utilizing seismic ground motion records from the Imperial Valley-06, Tokachi-Oki Aftershock, and Tokachi-Oki Mainshock earthquakes yielded a comprehensive evaluation of displacement and drift ratio fluctuations among various building categories. The findings indicate that structures with elevated height-to-width (H/L) ratios have increased displacement and drift ratios, underscoring the necessity for adequate separation distances according to structural attributes. Moreover, the study conforms to SNI 1726:2019, which stipulates that separation distances must account for maximal inelastic response displacement to mitigate seismic-induced damage. These findings provide essential insights for urban planners, structural engineers, and legislators in developing appropriate building rules and mitigation techniques to improve seismic resilience in Padang City. Future study may investigate sophisticated energy dissipation technologies or novel seismic dampers

to enhance building performance and mitigate pounding threats in densely populated urban areas.

Future Work

Based on the analysis conducted, it is recommended that the local government establish a minimum building separation distance of 1 meter in Padang City to prevent structural collisions during earthquakes and enhance seismic resilience. This guideline should be incorporated into urban planning regulations to ensure safer and more sustainable construction practices. Future studies should explore advanced seismic mitigation strategies, such as energy dissipation systems and base isolation, to further enhance building safety in earthquake-prone areas. Subsequent study ought to concentrate on investigating alternate seismic mitigation solutions, including energy dissipation systems, base isolation methods, and the incorporation of viscoelastic dampers. Furthermore, numerical modeling and practical investigations can substantiate the proposed separation distance criteria and enhance seismic performance characteristics. A cooperative initiative among municipal authorities, researchers, and construction experts is crucial for formulating extensive building rules that emphasize earthquake safety and urban resilience.

REFERENCE

[1] W. R. Kurnia, H. Haryani, and Y. Nori, "Kajian Perubahan Pengunaan Lahan serta Faktor-Faktor yang Mendorong Perubahan Pengunaan Lahan di Kecamatan Kuranji Kota Padang," Aug. 2020. Available at: https://ejurnal.bunghatta.ac.id/index.php/JFTSP/article/view/15758.

[2] S. Kumar and G. Jaiswal, "Study of pounding behavior between adjacent multi-storied buildings of varying heights by Time History Analysis method," *JETIR*, vol. 8, no. 10, pp. d189–d200, Oct. 2021. Available at: https://www.jetir.org/papers/JETIR2110322.pdf.

[3] S. Guérin-Marthe, P. Gehl, C. Negulescu, S. Auclair, and R. Fayjaloun, "Rapid earthquake response: The state-of-the art and recommendations with a focus on European systems," *International Journal of Disaster Risk Reduction*, vol. 52, p. 101958, Jan. 2021, Available at: https://doi.org/10.1016/j.ijdrr.2020.101958.

[4] S. Jiang, C. Zhai, and Y. Liu, "Experimental and numerical studies of seismic induced story-to-story and inter-story pounding," *Structures*, vol. 46, pp. 555–569, Dec. 2022, Available at: https://doi.org/10.1016/j.istruc.2022.10.061.

[5] B. T. Cayci and M. Akpinar, "Seismic pounding effects on typical building structures considering soil-structure interaction," *Structures*, vol. 34, pp. 1858–1871, Dec. 2021, Available at: https://doi.org/10.1016/j.istruc.2021.08.133.

[6] M. Miari, K. K. Choong, and R. Jankowski, "Seismic pounding between adjacent buildings: Identification of parameters, soil interaction issues and mitigation measures," *Soil Dynamics and Earthquake Engineering*, vol. 121, pp. 135–150, Jun. 2019, Available at: https://doi.org/10.1016/j.soildyn.2019.02.024.

[7] A. Tena-Colunga and D. Sánchez-Ballinas, "The collapse of Álvaro Obregón 286 building in Mexico City during the September 19, 2017 earthquake. A case study," *Journal of Building Engineering*, vol. 49, p. 104060, May 2022, Available at: https://doi.org/10.1016/j.jobe.2022.104060.

[8] M. Miari and R. Jankowski, "Analysis of pounding between adjacent buildings founded on different soil types," *Soil Dynamics and Earthquake Engineering*, vol. 154, p. 107156, Jan. 2022, Available at: https://doi.org/10.1016/j.soildyn.2022.107156.

[9] D. Isobe and T. Shibuya, "Preliminary numerical study on the reduction of seismic pounding damage to buildings with expanded polystyrene blocks," *Engineering*

Structures, vol. 252, p. 113723, Dec. 2021, Available at: https://doi.org/10.1016/j.engstruct.2021.113723.

[10] V. Follador, P. Carpanese, M. Donà, and F. da Porto, "Effect of retrofit interventions on seismic fragility of Italian residential masonry buildings," *International Journal of Disaster Risk Reduction*, vol. 91, p. 103668, Jun. 2023, Available at: https://doi.org/10.1016/j.ijdrr.2023.103668

[11] D. Oktiari and S. Manurung, "Model Geospasial Potensi Kerentanan Tsunami Kota Padang," *Jurnal Meteorologi dan Geofisika*, vol. 11, no. 2, Dec. 2010, Available at: https://doi.org/10.31172/jmg.v11i2.73.

[12] R. Apdeni *et al*., "Application of ground penetrating radar for evaluating foundation structure condition after earthquake," *Teknomekanik*, vol. 7, no. 1, pp. 85–100, Jun. 2024, Available at: https://doi.org/10.24036/teknomekanik.v7i1.26772.

[13] BPBD Kota Padang, "Mengenang Gempa 2009 di Kota Padang". Feb. 2009. Available at: https://bpbd.padang.go.id/konten/mengenang-gempa-2009-di-kota-padang.

[14] F. A. Chairunnisa, "Evaluasi Kinerja Struktur Bangunan Rumah Toko Eksisting Pada Daerah Rawan Bencana Gempa Bumi," Universitas Andalas. Apr. 2022. Available at: http://scholar.unand.ac.id/102807/.